



Plant toxic and non-toxic nature of organic dyes through adsorption mechanism on cellulose surface

Natesan Buvaneswari^a, Chellapandian Kannan^{b,*}

^a Department of Chemistry, Periyar University, Salem-636011, Tamil Nadu, India

^b Department of Chemistry, Manonmanium Sundaranar University, Abishekapatti, Thirunelveli-627012, India

ARTICLE INFO

Article history:

Received 31 July 2010

Received in revised form

10 November 2010

Accepted 14 February 2011

Available online 22 February 2011

Keywords:

Brinjal plant root

Malachite green

Methyl orange

Adsorption mechanism

ABSTRACT

Effluents releasing from dyeing industries directly affect the soil, water, plant and human life. Among these dyes, plant poisoning, soil polluting and water polluting nature of organic dyes are not yet identified. The plant poisoning and non-poisoning organic dyes are identified through adsorption mechanism of cationic malachite green (MG) and anionic methyl orange (MO) on brinjal plant root powder (cellulose). The positive ΔH° (44 kJ mol^{-1}) of MG higher than 40 kJ mol^{-1} confirmed the adsorption of MG on cellulose is chemisorption and the negative ΔH° (-11 kJ mol^{-1}) less than 40 kJ mol^{-1} showed that the adsorption of MO on cellulose is physisorption. The ΔG° values for the adsorption of MG and MO on BPR are not much increased with increase of temperature which indicated that the adsorption is independent of the temperature. The entropy change for the adsorption of MG and MO has proved that the MG ($+\Delta S^\circ$) has less disorder at the adsorption interface and MO ($-\Delta S^\circ$) has the high disorder at the adsorption interface.

The recovery of both dyes has been studied in water at 80°C on BPR surface and observed that the MO recovery is 95% and MG is 10%. The poor desorption of MG is due to the strong chemisorption on BPR (cellulose) surface proves its plant poisoning nature. The high recovery of MO due to physisorption mechanism proves that MO is not poisoning the plant.

© 2011 Elsevier B.V. All rights reserved.

1. Introduction

Dye waste water from textile dyeing and dye manufacturing industries cause serious pollution problems. The dye effluents discharged into water bodies like lakes, rivers, etc. affect the aquatic flora and fauna and cause many water borne diseases [1]. Since synthetic dyes are complex aromatic compounds, they are more stable and more difficult to biodegradation. "Now-a-days, there are more than 10,000 types of dyes available commercially. The annual production of dyes worldwide is around 7×10^5 tonnes; 10–15% of the dyes are discharged into water bodies as effluents" [32,33]. The conventional dye effluent treatment methods like coagulation, flocculation, oxidation, photochemical destruction, ion exchange and membrane filtration are costly and require some additional chemicals [2,3]. Hence, these methods are not much suitable to treat organic dye effluents. The adsorption methods have been widely used for the removal of colorants from waste water. Adsorbents like acid activated carbon, *Prosopis cineraria* sawdust, micro- and mesoporous rice husk-based active carbon, de-oiled soya, hen feathers,

neem leafs and mesoporous aluminophosphate molecular sieves have been used for the dyes removal [4–10]. But, these methods are not able to identify the plant poisoning, soil polluting and water polluting organic dyes.

Malachite green adsorption studies are reported in tetrahedral silica and non-tetrahedral alumina, baggasse fly ash and activated carbon, CZn5, PETNa8, activated carbon from lignite, activated charcoal, ground nut shell waste, sugarcane baggasse, waste material from paper industry, pine bark, ash, silk cotton hull, sago waste, maize cob and coconut tree saw dust [11–22].

Methyl orange adsorption studies are reported on carboxylated diaminoethane sporopollenin [23], raw and acid activated montmorillonite in fixed beds [24], starches [25], calcined layered double hydroxides [26], and crude drug starches [27].

However, there is no report in the literature to identify the plant toxic and non-toxic organic dyes. Hence, attempts have been made to adsorb cationic MG and anionic MO on brinjal plant root powder (cellulose surface) to evaluate the plant toxic nature of organic dyes through adsorption mechanism [28] from aqueous solution.

Novelty of the present investigation (the removal of MG and MO from aqueous solution) is to evaluate the toxic effect of organic dyes on plants and to classify dyes into the plant toxic and nontoxic types of organic dyes. The study has been carried out over plant roots, because the root is the base for all living plants and also the material is not yet used as an adsorbent for the removal of organic

* Corresponding author. Tel.: +91 462 2338721/2333741;

fax: +91 462 2322973/2334363.

E-mail addresses: buviechem@gmail.com (N. Buvaneswari), chellapandiankannan@gmail.com (C. Kannan).

dyes. Moreover, the plant root contains 98% cellulose; hence, the study has been carried out over plant root powder to understand the mechanism of toxic effect of organic dyes to plants.

2. Experimental

2.1. Materials

The dyes used in this study are malachite green (Merck India Ltd, molecular formula $(C_{24}H_{25}N_2O_2)_2 \cdot 2C_2H_2O_4$, molecular weight 837.02 and λ_{max} 616–620 nm) and methyl orange (Merck India Ltd, molecular formula $C_{14}H_{14}N_3NaO_3S$, molecular weight 327.33, C.I. 13025). The adsorbent used in this study is BPR powder. The brinjal plant roots (BPRs) are collected from agricultural wastes and dried in sunlight and grinded well. The structure of malachite green and methyl orange used in these studies are shown in Figs. 1 and 2 respectively.

2.2. Preparation of stock solutions of MG and MO

The stock solutions of MG and MO (1000 mg L^{-1}) are prepared by dissolving 1 g of dyes MG and MO in standard measuring flasks separately by using double distilled water. The working solutions of desired concentrations are prepared by successive dilutions of stock solutions. The dye concentration is analyzed by UV-Spectrophotometer (Perkin Elmer, Lambda 25).

2.3. Batch adsorption studies

Dried BPR powder (0.25 g) is added to 50 ml of MG and MO solutions in 100 ml conical flasks separately. The solutions are stirred on magnetic stirrer (Remi-Model-1MH) and at the end of the experiment, the solutions are centrifuged off. The final concentrations of the solutions are measured spectrophotometrically. The contact time has been studied up to one hour to find out the adsorption equilibrium. The concentration effect of MG and MO on BPR is studied in the concentration range of $100\text{--}600 \text{ mg L}^{-1}$. The temperature effect of MG and MO are studied in the range of $40\text{--}70^\circ\text{C}$ [29]. The adsorbent dosage effect is also studied in the range of $200\text{--}1000 \text{ mg}$.

2.4. Desorption studies

The dyes (MG and MO) adsorbed BPR is used in the desorption studies. 200 mg of MG adsorbed BPR and MO adsorbed BPR are added with 50 ml of water in 100 ml conical flasks separately. The solutions are stirred for one hour at 80°C in a magnetic stirrer (Remi-Model MLH). At the end of the experiment, the solutions

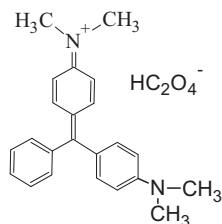


Fig. 1. Structure of malachite green.

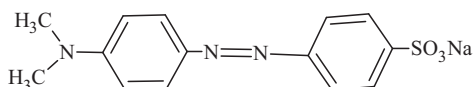


Fig. 2. Structure of methyl orange.

are centrifuged off. The final concentrations of the solutions are measured spectrophotometrically.

3. Result and discussion

3.1. Contact time and adsorption mechanism

The effect of contact time for adsorption shows rapid adsorption equilibrium is attained within 25 min for MG and for MO within 30 min and further increase of contact time does not increase the adsorption (Fig. 3). The removal of MG is 91% and MO is 38%. The higher adsorption of MG indicates the adsorption of cationic MG with $-\text{OH}$ group of BPR (cellulose-98%) is chemisorption [30] shown in Fig. 4. But the less adsorption of MO is due to charge repulsion between the anionic MO and basic $-\text{OH}$ group of cellulose. However, the low adsorption of MO on cellulose surface is due to the physisorption is shown in Fig. 5.

3.2. Effect of initial dye concentration

The effect of dye concentration is studied in the range of $100\text{--}600 \text{ ppm}$ for MG and MO on BPR is shown in Fig. 6. It is found that percentage adsorption of MG decreased with increase in initial dye concentration from 91 to 72%. However, percentage adsorption of MO decreased with the increase in initial dye concentration $38\text{--}27\%$. This may be due to saturation of active sites and surface area on the surface of the BPR.

3.3. Effect of pH

The pH effect on the adsorption of MG and MO on BPR powder is shown in Fig. 7. The pH of MG and MO dyes varied from 2 to 10. It can be seen that cationic MG dye adsorption was low at $\text{pH} < 4$. The decrease in the adsorption at low pH may be attributed to two reasons. At low pH, the number of negatively charged adsorbent sites decreased and the number of positively charged surface sites increased, which did not favour the adsorption of positively charged dye cations due to electrostatic repulsion. Secondly lower adsorption of MG at acidic pH is due to the presence of excess H^+ ions competing with dye cations for the adsorption sites of BPR. Adsorption of MG and MO on BPR increased with increase of pH up to 6. The optimum value of pH for both dyes adsorption on BPR is 6. Above pH 6, adsorption percentage decreases.

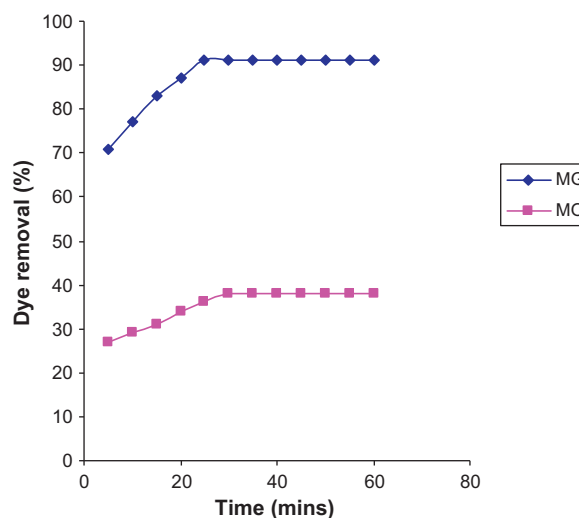


Fig. 3. Effect of contact time for the uptake of dyes on BPR. Temperature 30°C , concentration 100 ppm , BPR dosage $250 \text{ mg}/50 \text{ ml}$.

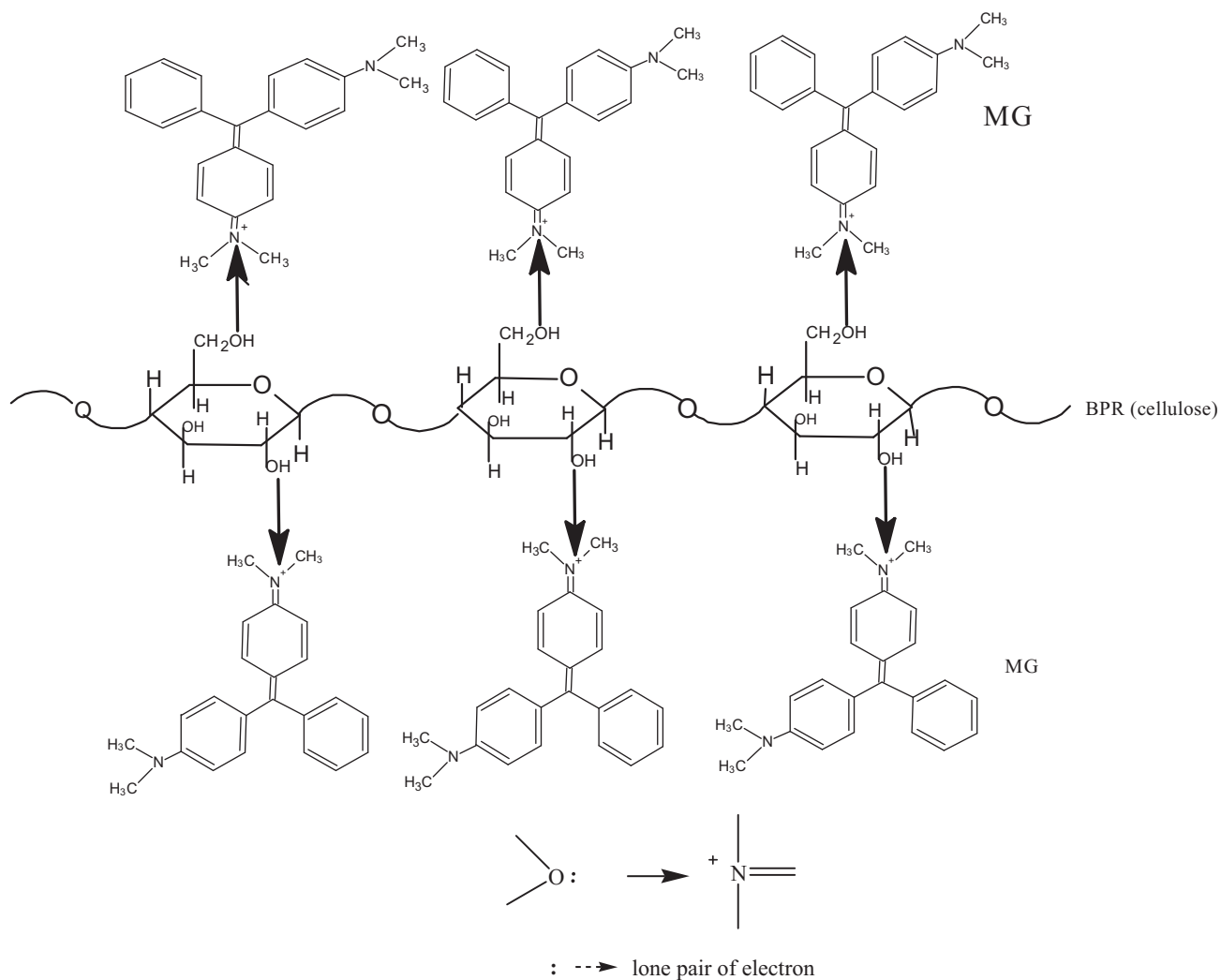


Fig. 4. Adsorption (chemisorption) mechanism of cationic malachite green on cellulose (BPR) surface. The lone pair of electron present on the oxygen atom (cellulose) shifted towards the positive charge present on the nitrogen atom of the MG. This shifting of electron is known as chemisorption.

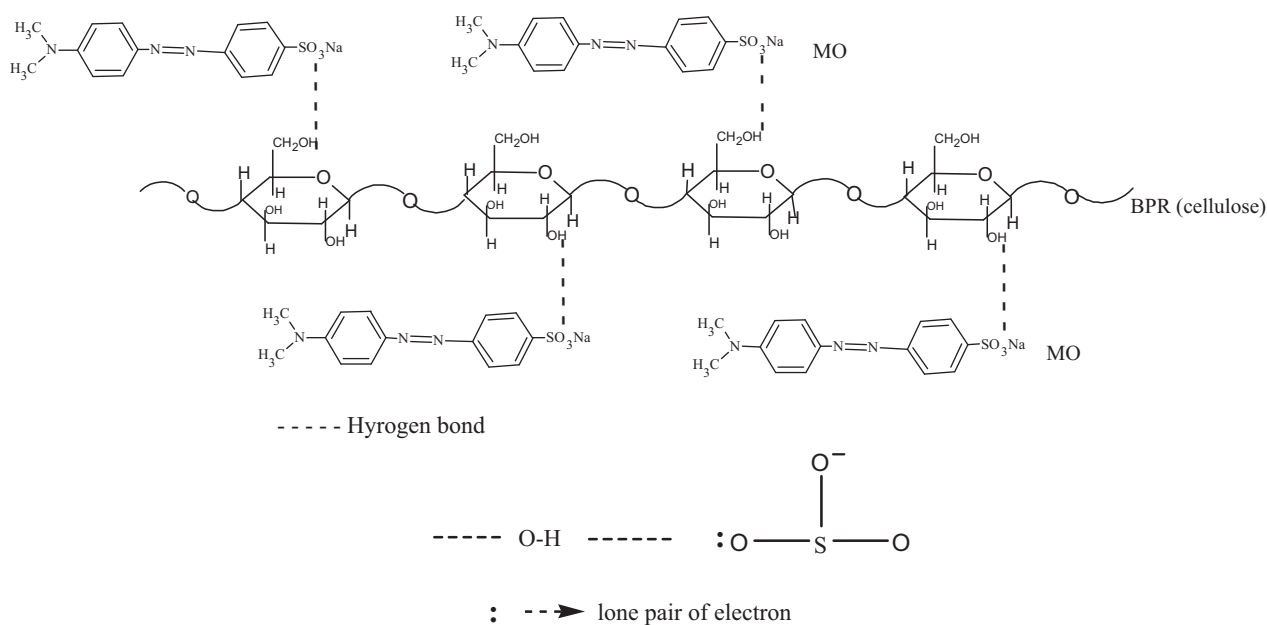


Fig. 5. Adsorption (physisorption) mechanism of anionic methyl orange on cellulose (BPR). Physical force of attraction between the hydrogen present in cellulose (-OH) and the oxygen present in the MO (-SO₃⁻). This type of weak adsorption is known as physisorption.

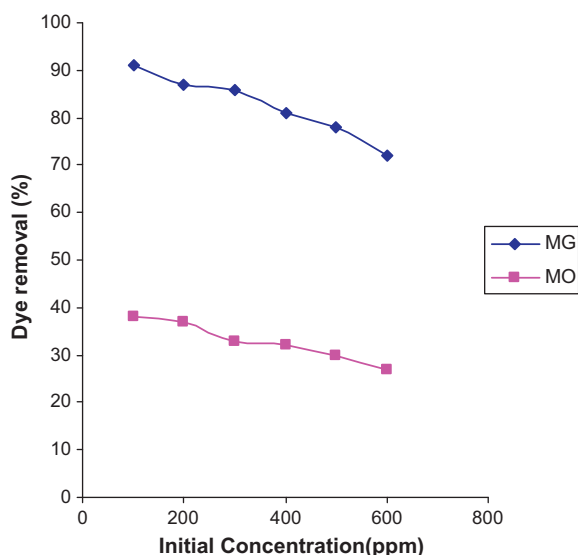


Fig. 6. Effect of initial dye concentration for the uptake of dyes MG and MO on BPR. Temperature 30 °C, BPR dosage 250 mg, time 25 min for MG and 30 min for MO.

3.4. Effect of temperature

The effect of temperature for the uptake of dyes on BPR at 30–70 °C is shown in Fig. 8. Percentage adsorption of MG is found to increase with increase of temperature due to the increase of charge interaction between the basic sites of BPR and cationic MG (Fig. 3). On the other hand, the adsorption of MO slightly increased up to 40 °C and further increase of temperature decreases the adsorption that may be due to the collapse of hydrogen bond (Fig. 4) or physisorption of MO on BPR surface.

3.5. Effect of adsorbent dosage

The effect of adsorbent dosage on the adsorption of dyes is shown in Fig. 9. The percentage adsorption of dyes found to increase with increase of BPR dosage. This is due to the increase in the number of valuable adsorption sites as well as the surface area with increasing adsorbent dosage.

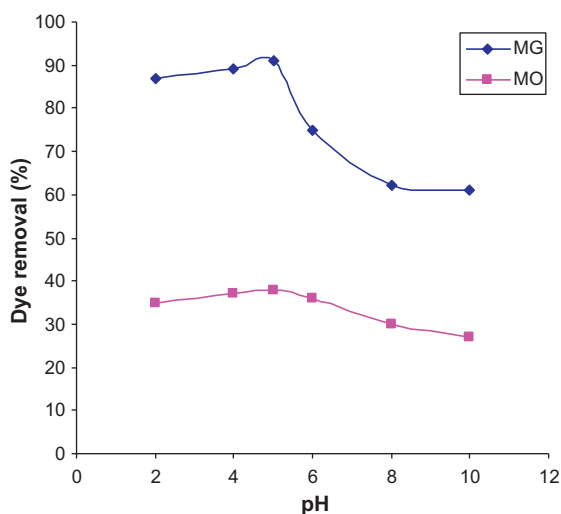


Fig. 7. Effect of pH on the uptake of anionic dyes on BPR. Temperature 30 °C, BPR dosage 250 mg/50 ml, time 25 min for MG and 30 min for MO.

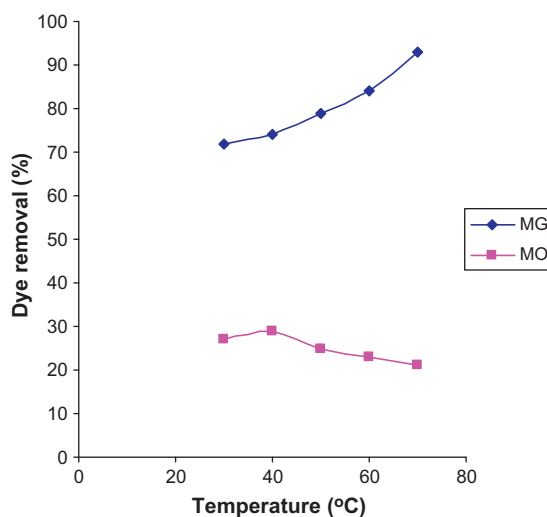


Fig. 8. Effect of temperature for the uptake of MG and MO on BPR. Concentration 600 ppm, time 25 min for MG and 30 min for MO, BPR dosage 250 mg/50 ml.

3.6. Adsorption isotherms

The adsorption isotherm indicates how the dye molecules distribute between the liquid phase and the solid phase when the adsorption process reaches an equilibrium state. The analysis of the isotherm data by fitting them to different isotherm models is an important step to find the suitable model that can be used for designing the adsorption purpose.

The Langmuir and Freundlich are the most frequently employed models to describe the experimental data of adsorption isotherms. In this investigation, both models are used to describe the relationship between the monolayer and multilayer adsorption process at equilibrium.

Adsorption isotherm of MG and MO dyes on BPR at different concentrations are studied and observed that both are well matched with the Langmuir and Freundlich adsorption isotherms.

3.6.1. Langmuir adsorption isotherm

The Langmuir plot for the adsorption of MG and MO are given in Fig. 10a and b respectively. The Langmuir adsorption parameters

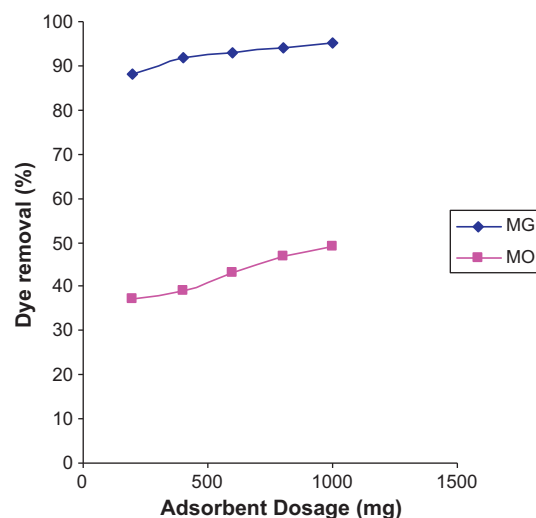


Fig. 9. Effect of adsorbent dosage for the uptake of dyes on BPR. Concentration 600 ppm, time 25 min for MG and 30 min for MO, temperature 30 °C.

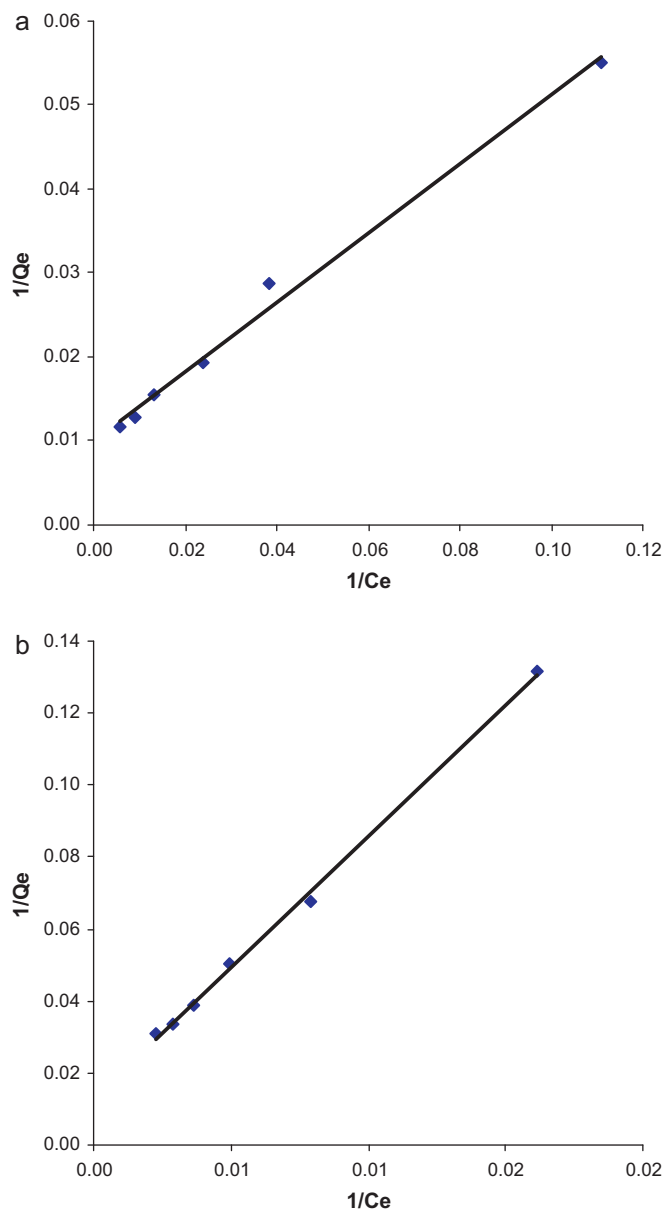


Fig. 10. Vant Hoff's plot for the adsorption of dyes on BPR. (a) Langmuir adsorption isotherm for the adsorption of MG on B PR. (b) Langmuir adsorption isotherm for the adsorption of MO on BPR.

are given in Table 1. The R^2 value is near 1 for both dyes indicate that the adsorption follows the Langmuir adsorption isotherm. The monolayer capacity for MG is more than MO (Table 1). This is one of the supporting evidence for heavy toxicity of cationic MG than anionic MO to plants.

3.6.2. Freundlich adsorption isotherm

The Freundlich plot for the adsorption of MG and MO are given in Fig. 11a and b respectively. The various parameters obtained from

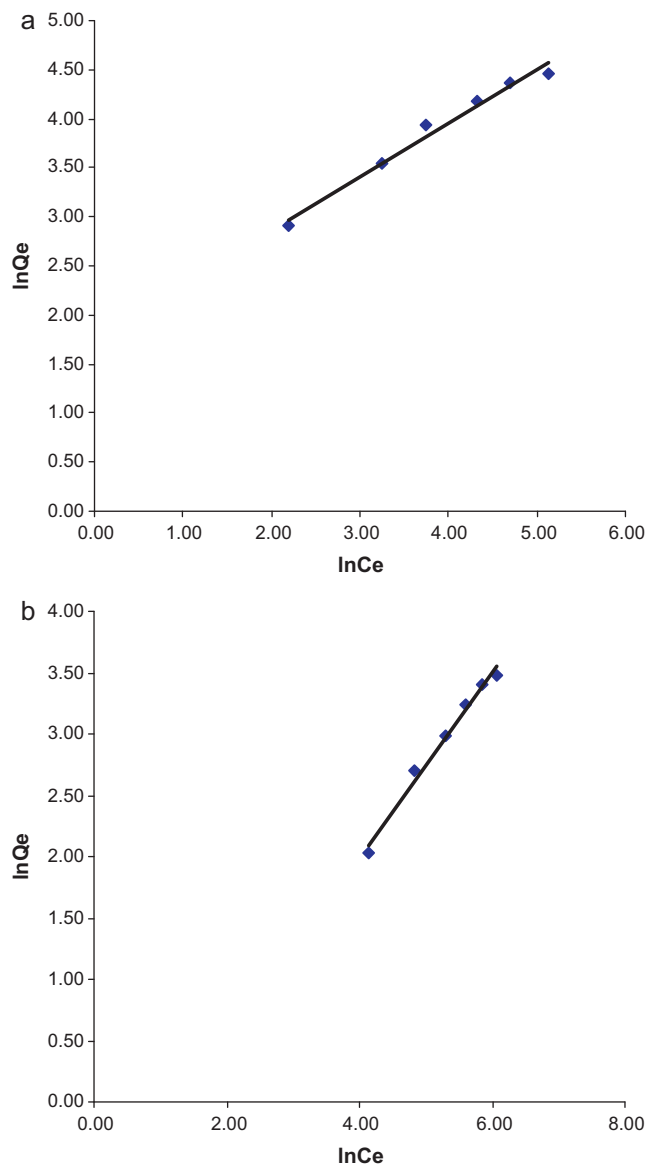


Fig. 11. (a) Freundlich adsorption isotherm for adsorption of MG on BPR. (b) Freundlich adsorption isotherm for adsorption of MO on BPR.

Freundlich adsorption isotherms are given in Table 1. The R^2 value for the both adsorption model of MG ad MO on BPR powder close to 1 (Table 1) indicates that the adsorption of cationic and anionic dyes followed Freundlich adsorption isotherm. The number of layer (n) of adsorption of MG is 2 and for MO is 1 (Table 1). The cationic MG adsorbed on BPR is more than 1 corresponds to multilayer adsorption, but MO has monolayer adsorption. This is another evidence for heavy loading of cationic MG than anionic MO and it confirms that the MG toxicity to plant root is more than MO.

Table 1
Adsorption isotherm and kinetics for adsorption of MO and MG on BPR.

| Dyes | K_2 ($\text{g mg}^{-1} \text{ min}$) | Freundlich adsorption isotherm | | | Langmuir adsorption isotherm | | |
|------|------------------------------------------|--------------------------------|------------|-------|------------------------------|-----|-------|
| | | Q_{max} (mg/g) | b (L/mg) | R^2 | K_F (L/g) | n | R^2 |
| MG | 1.589×10^{-2} | 100.29 | 0.0242 | 0.992 | 5.91 | 2 | 0.979 |
| MO | 3.660×10^{-2} | 78.43 | 0.0017 | 0.998 | 0.37 | 1 | 0.988 |

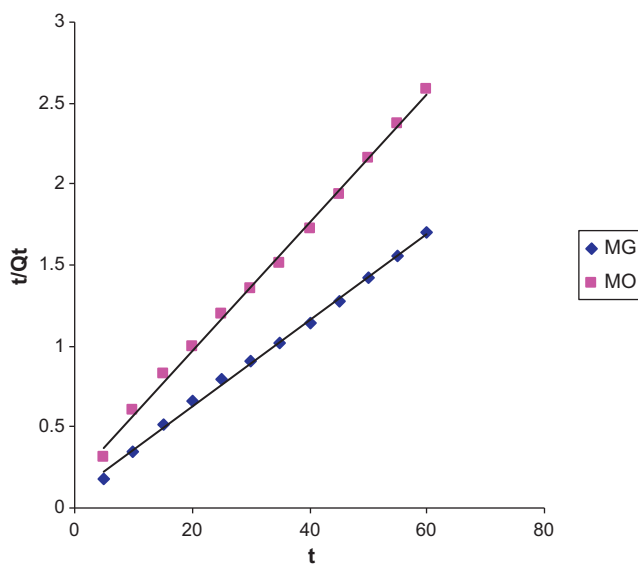


Fig. 12. Kinetic studies for the adsorption of dyes on BPR.

3.7. Adsorption kinetics

The fast of the adsorption processes can be calculated from the knowledge of kinetic studies. The adsorption kinetics of MG and MO on BPR powder has been studied in regular time interval at room temperature to determine the kinetics of the adsorption. In order to examine the controlling mechanism of the adsorption process, pseudo-first order and pseudo-second order equations are used to test the kinetics of adsorption. A simple kinetic analysis of adsorption is the pseudo-first order rate expression of the Lagergren equation. The first order kinetics only describes the sorption sites and not the adsorption process as a whole.

3.7.1. Lagergren pseudo-first-order model

The simple Lagergren pseudo-first-order model assumes that the rate of change of solute uptake with time is directly proportional to the difference in the amount of solute adsorbed at time of equilibrium Q_e (mg g^{-1}) and the amount of solute adsorbed at any time, Q_t (mg g^{-1}):

Pseudo-first-order model has been described by Lagergren is given by

$$\ln(Q_e - Q_t) = \ln Q_e - k_1 t$$

where Q_e is the amount of adsorbate adsorbed at equilibrium (mg g^{-1}), Q_t is the amount of adsorbate adsorbed at time t (mg g^{-1}), k_1 is the first order rate constant (min^{-1}), and t is time in min.

To verify Lagergren's pseudo first order kinetics, graphs between time versus $\log(Q_e - Q_t)$ are plotted for the adsorption of MG and MO on BPR powder.

3.7.2. Pseudo-second-order model

The pseudo-second-order equation based on adsorption equilibrium capacity is expressed as follows,

$$\frac{t}{Q_t} = \frac{1}{k_2 Q_e^2} + \frac{1}{Q_e} t$$

where k_2 is the second-order rate constant ($\text{g mg}^{-1} \text{min}^{-1}$), Q_e is the amount of solute adsorbed on the surface at equilibrium (mg g^{-1}), and Q_t is the amount of solute adsorbed at time t (mg g^{-1}).

The plot of t/Q_t versus t gives straight lines for cationic and anionic dyes adsorption on BPR. The Q_e and k_2 can be calculated from the slope and intercept of the plots (Fig. 12). The Q_e , k_2 , R^2

Table 2

Thermodynamic parameters for uptake of MO and MG on BPR.

| Dyes | 1/T (K) | ΔG° (kJ/mole) | ΔH° (kJ/mole) | ΔS° (J/mole K) |
|------|---------|----------------------------|----------------------------|-----------------------------|
| MG | 0.0033 | -2.3804 | 43.27 | -88.47 |
| | 0.0032 | -3.1458 | | |
| | 0.0031 | -4.0739 | | |
| | 0.0030 | -5.0280 | | |
| | 0.0029 | -9.0668 | | |
| MO | 0.0033 | 2.5068 | -8.31 | 30.66 |
| | 0.0032 | 2.3312 | | |
| | 0.0031 | 2.9516 | | |
| | 0.0030 | 3.3468 | | |
| | 0.0029 | 3.7799 | | |

values are given in Table 2. The linear regression coefficient near to 1 ($R^2 = 0.999$) indicates that the adsorption followed the pseudo-second order kinetics (Fig. 12) model. The results are also tested with a pseudo-first order kinetics (Fig. 12) model, but the R^2 value is less than 1 indicates that adsorption of cationic MG and anionic MO dyes on BPR are not perfectly follows the pseudo-first order kinetics (Table 1).

Even though pseudo-first-order model has provided good fit at early stages, the experimental data have shown considerable deviation at later times. However, pseudo-second-order model has shown almost perfect fit ($R^2 = 0.999$) in the whole range of considered time. This fit of the pseudo-second order kinetic model suggests that the model can be efficiently used to predict the kinetics of adsorption of MG and MO on BPR. Since this model is based on the adsorption capacity, it will help to predict the adsorption behavior over the whole range of concentration and supporting chemisorption as rate controlling mechanism. Chemisorption usually indicates that the adsorption process is irreversible. Views of similar kind have been put forward by other workers. This proposed irreversible adsorption process should be better supported using desorption experiments and by measuring the free energy (ΔG°) of adsorption.

3.8. Adsorption thermodynamics

The changes in adsorption processes that can be expected during the process require the brief idea of thermodynamic parameters. The concept of thermodynamic assumes that in an isolated system where energy cannot be gained or lost, the entropy change is the driving force [31]. The thermodynamic parameters [34] that must be considered to determine the process are enthalpy of adsorption (ΔH°), free energy change (ΔG°) and entropy change (ΔS°) due to transfer of unit mole of solute from solution onto the solid-liquid interface. The important thermodynamic function ΔH° is very useful whenever a differential change occurs in the system. The negative value of ΔH° indicates that adsorption process is exothermic process and positive value indicates that adsorption is endothermic process. The other important thermodynamic parameters are the change in entropy ΔS° . The parameter ΔS° is used to identify the spontaneity in the adsorption process.

Thermodynamic parameters such as change in free energy (ΔG°) kJ mol^{-1} , enthalpy (ΔH°) kJ mol^{-1} and entropy (ΔS°) $\text{JK}^{-1} \text{mol}^{-1}$ are determined using the following equations. The enthalpy and entropy can be calculated from Van't Hoff plot as shown in Fig. 10. The ΔG° , ΔH° and ΔS° values calculated for the adsorption of MG and MO are given in Table 2.

The Gibbs free energy change of the adsorption process is related to the equilibrium constant by the classic Van't Hoff equation. The equation is

$$\Delta G^\circ = -RT \ln K_c$$

where ΔG^0 is free energy of activation (kJ/mol), R is the universal gas constant ($8.314 \text{ J K}^{-1} \text{ mol}^{-1}$), T is temperature (K), and K_c is equilibrium constant of adsorption.

The equilibrium constant (K_c) calculated from the following equation

$$K_c = \frac{C_{Ae}}{C_e}$$

where C_{Ae} is the adsorbed dye concentration at equilibrium and C_e is the equilibrium concentration of dye in solution.

By substituting all values in Gibb's free energy equation, ΔG^0 can be calculated and the values are given in Table 2.

The negative ΔS^0 values for the adsorption of MG have shown the less disorder at the adsorption interface. The ΔG^0 values not much alters with increase of temperature indicates that the adsorption is more in room temperature. The positive value of ΔH^0 more than 40 kJ mol^{-1} indicates that the MG adsorption is chemisorption [28,35,37].

The positive ΔS^0 values for adsorption of MO have shown high disorder at the adsorption interface. The negative value of ΔH^0 less than 40 kJ mol^{-1} indicates that the MO adsorption is physisorption [36,38] on BPR surface. Because BPR surface is negative, the anionic MO is not able to chemisorb on the BPR surface.

3.9. Dye recovery

Desorption of MG and MO is carried out at 80°C in water separately. The MO recovery is 95% and MG is 10%. This is proved by the strong adsorption of MG on cellulose surface. This is an additional evidence for the chemisorption of MG and physisorption of MO on cellulose surface (Figs. 3 and 4) and also is a supportive evidence to classify that the cationic MG is plant toxic and the anionic MO is non-toxic to plants.

4. Conclusion

The rapid adsorption equilibrium is attained for MG and MO adsorption on BPR (cellulose) surface within 35 min. The adsorption capacity of MG was more than MO on BPR (cellulose) surface. The adsorption thermodynamics of MG proves that the adsorption is chemisorption on basic surface of cellulose (BPR) and MO adsorption is physisorption. The recovery of MG in water is very poor and MO is very high. Thus, the rapid adsorption and poor recovery, due to chemisorption mechanism on cellulose surface, proved that the MG is a plant toxic organic dye. The high recovery of MO, due to physisorption mechanism on cellulose surface, proved the non-toxic nature to plant. The present investigation proves that the cationic MG is plant toxic and anionic MO non-toxic to plant. Thus, the study may open a new research avenue in environmental science to classify the plant toxic and non-toxic organic dyes.

References

- [1] S.J. Allen, B. Koumanova, Decolorisation of water/wastewater using adsorption, *J. Univ. Chem. Technol. Metall.* 40 (2005) 175–195.
- [2] D. Roy, K.T. Valsaraj, S.A. Kottai, Separation of organo dyes from wastewater by using colloidal gas apherons, *Sep. Purif. Technol.* 27 (1992) 573–588.
- [3] D. Pak, W. Chang, Color and suspended solid removal with a novel coagulation Technology, *Water Sci. Technol.: Water Supply* 2 (2002) 77–81.
- [4] M. Hema, S. Arivoli, Comparative study on the adsorption kinetics and thermodynamics of dyes onto acid activated low cost carbon, *Int. J. Phys. Sci.* 2 (2007) 010–017.
- [5] V.K. Garg, R. Kumar, R. Gupta, Removal of malachite green dye from aqueous solution by adsorption using agro-industry waste: a case study of *Prosopis cineraria*, *Dyes Pigm.* 62 (2004) 1–10.
- [6] Y. Guo, S. Yang, W. Fu, J. Qi, R. Li, Z. Wang, H. Xu, Adsorption of malachite green on micro- and mesoporous rice husk-based active carbon, *Dyes Pigm.* 56 (2003) 219–229.
- [7] A. Mittal, L. Krishnan, V.K. Gupta, Removal and recovery of malachite green from wastewater using an agricultural waste material, de-oiled soya, *Sep. Purif. Technol.* 43 (2005) 125–133.
- [8] A. Mittal, Adsorption kinetics of removal of a toxic dye, malachite Green, from wastewater by using hen feathers, *J. Hazard. Mater.* 133 (2006) 196–202.
- [9] C. Kannan, K. Iyyappan, A. Anitha, Malachite green and methyl orange dye removal from aqueous solution by adsorption onto neem leaves, in: International Conference on Materials for the Millennium, Department of Applied Chemistry, CUSAT, Kochi, 2007, pp. 94–95.
- [10] A. Selvaraj, T.T. Sundaram, N. Buvanewari, C. Kannan, Synthesis and characterisation of mesoporous aluminosilicate molecular sieves and adsorption application, in: International Conference on Materials for the Millennium, Department of Applied Chemistry, CUSAT, Kochi, 2007, pp. 28–29.
- [11] C. Kannan, T.T. Sundaram, T. Palvannan, Environmentally stable adsorbent of tetrahedral silica and non-tetrahedral alumina for removal of malachite green dye from aqueous solution, *J. Hazard. Mater.* 157 (2008) 137–145.
- [12] C. Kannan, T.T. Sundaram, T. Palvannan, Soil pollution by malachite green dye and dye recovery from effluent, *Environ. Sci. Indian J.* 2 (2007) 10–16.
- [13] Indra Deo Mall, Vimal Chandra Srivastava, Nitin Kumar Agarwal, Indra Mani Mishra, Adsorptive removal of malachite green dye from aqueous solution by bagasse fly ash and activated carbon-kinetic study and equilibrium isotherm analyses, *Colloids Surf. A: Physicochem. Eng. Aspects* 264 (2005) 17–28.
- [14] C. Akmil-Basar, Y. Onal, T. Kilicer, D. Eren, Adsorptions of high concentration malachite green by two activated carbons having different porous structures, *J. Hazard. Mater.* 127 (2005) 73–80.
- [15] Y. Onal, C. Akmil-Basar, C. Sarici-Ozdemir, Investigation kinetics mechanisms of adsorption malachite green onto activated carbon, *J. Hazard. Mater.* 146 (2007) 194–203.
- [16] M.J. Iqbal, M.N. Ashiq, Adsorption of dyes from aqueous solutions on activated charcoal, *J. Hazard. Mater.* 139 (2007) 57–66.
- [17] R. Malik, D.S. Ramteke, S.R. Wate, Adsorption of malachite green on groundnut shell waste based powdered activated carbon, *Waste Manag.* 27 (2007) 1129–1138.
- [18] A.G. Liew Abdullah, M.A. Mohd Salleh, M.K. Sili Mazlina, M.J. Megat Mohd Noor, M.R. Osman, R. Wagiran, S. Sobri, Azo dye removal by adsorption using waste biomass: sugarcane bagasse, *Int. J. Eng. Technol.* 2 (2005) 8–13.
- [19] A. Mendez, F. Fernandez, G. Gasco, Removal of malachite green using carbon based adsorbents, *Desalination* 206 (2007) 147–153.
- [20] V.K. Gupta, A. Mittal, L. Krishnan, V. Gajbe, Adsorption kinetics and column operations for the removal and recovery of malachite green from waste water using ash, *Sep. Purif. Technol.* 40 (2004) 87–96.
- [21] K.V. Kumar, V. Ramamurthi, S. Sivanesan, Biosorption of malachite green cationic dye onto pithoporia sp., a fresh water algae, *Dye Pigm.* 69 (2006) 74–79.
- [22] V.K. Garg, R. Gupta, A.B. Vadar, R. Kumar, Dye removal from aqueous solution by adsorption on treated dust, *Bioresour. Technol.* 89 (2003) 21–24.
- [23] A. Ayar, O. Gezici, M. Kuçukosmanoglu, Adsorptive removal of Methylene blue and Methyl orange from aqueous media by carboxylated diaminoethane sporopollenin: on the usability of an aminocarboxylic acid functionality-bearing solid-stationary phase in column techniques, *J. Hazard. Mater.* 146 (2007) 186–193.
- [24] Min-Yu Teng, Su-Hsia Lin, Removal of methyl orange dye from water onto raw and acidactivated montmorillonite in fixed beds, *Desalination* 201 (2006) 71–81.
- [25] T. Boki Imai, S. Ohno, Adsorption of methyl orange on starches, *J. Food Sci.* 56 (1991) 90–92.
- [26] Z.M.S.J. Ni, L.G. Wang, F.F. Xing, G.X. Pan, Treatment of methyl orange by calcined layered double hydroxides in aqueous solution: adsorption property and kinetic studies, *J. Colloid Interface Sci.* 316 (2007) 284–291.
- [27] Y. Yamada, K. Boki, A. Matsuyama, M. Takahashi, M. Iwaki, Adsorption of cationic methylene blue and anionic methyl orange by crude drug starches, *J. Appl. Glycosci.* 52 (2005) 101–106.
- [28] C. Kannan, N. Buvanewari, T. Palvannan, Removal of plant poisoning dyes by adsorption on tomato plant root and green carbon from aqueous solution and its recovery, *Desalination* 249 (2009) 1132–1138.
- [29] S. Sivamani, C. Parvathi, C. Prakash, C.V. Koushik, Removal of malachite green from its aqueous solution by Pithoporia sp., *J. Adv. Biotechnol.* VIII (2009) 32–34.
- [30] C. Kannan, N. Buvanewari, T. Palvannan, Removal of plant poisoning dyes by adsorption on tomato plant root and green carbon from aqueous solution and its recovery, *Desalination* 249 (3) (2009) 1132–1138.
- [31] L.C. Juang, C.C. Wang, C.K. Lee, Adsorption of basic dyes onto MCM-41, *Chemosphere* 64 (2006) 1920–1928.
- [32] P. Sine, *Synthetic Dyes*, Rajat Publications, New Delhi, 2003, West Ed.
- [33] R. Wilfred Sugumar, Sandhya Sadanandan, Combined anaerobic-aerobic bacterial degradation of dyes, *E-J. Chem.* 7 (3) (2010) 739–744.
- [34] Z. Zawani, A. Luqman Chuah, T.S.Y. Choong, Equilibrium, kinetics and thermodynamic studies: adsorption of remazol black 5 on the palm kernel shell activated carbon (PKS-AC), *Eur. J. Sci. Res.* 37 (2009) 67–76.
- [35] A.T. Mohd Din, B.H. Hameed, Adsorption of methyl violet dye on acid modified activated carbon: isotherms and thermodynamics, *J. Appl. Sci. Environ. Sanit.* 5 (2010) 161–170.
- [36] Y. Seki, K. Yurdakoc, Equilibrium, kinetics and thermodynamic aspects of promethazine hydrochloride sorption by iron rich smectite, *Colloids Surf. A: Physicochem. Eng. Aspects* 340 (2009) 143–148.
- [37] S. Arivoli, M. Hema, P. Martin Deva Prasath, Adsorption of malachite green onto carbon prepared from borassus bark, *Arabian J. Sci. Eng.* 34 (2009) 31–42.
- [38] P. Sivakumar, P.N. Palanisamy, Adsorption studies of basic red 29 by a non-conventional activated carbon prepared from euphorbia antiquorum 1, 1 (2009) 502–510.